Nuclear Observable For Nuclear Processes

GIRY Aurélien

Université de Strasbourg

Supervisor : Kamila Sieja

Table of contents

Nuclear astrophysics

Nucleosynthesis : All the processes that create the elements in our universe and the influence of the astrophysical conditions on the properties of these processes.
We will consider the **explosive nucleosynthesis**, which are the processes occurring under extreme conditions and more specifically the r-process. It occurs at **large neutron densities** and at high temperatures.
It creates about half of $A \approx 60$. It follows an isotopic chain until a $(n, \gamma) \leftrightarrow (\gamma, n)$ equilibrium with $(n, \gamma) : A + n \rightarrow B + \gamma$

Hauser-Feshbach

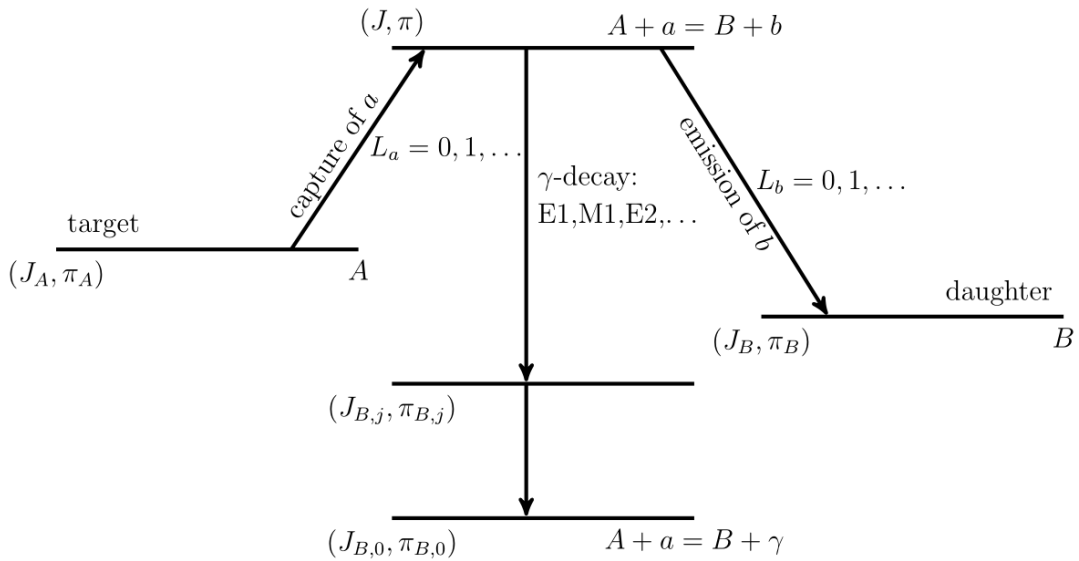

Figure 1: Scheme of a Hauser-Feshbach reaction, ie. $A + a \rightarrow$ highly excited compound nucleus $\rightarrow B + b$, taken from Ref. [1]. We define the Q-value as : $Q = m_a + m_A - (m_b + m_B)$

Conservation laws : $E_{CN} = E_A + E_a - Q$; $|J_A - I| \leq J \leq J_A + I$; $\pi = (-1)^L \pi_A$ (X=electric) or $\pi = (-1)^{L-1} \pi_A$ (X=magnetic)

Cross-section of neutron capture rate

The cross-section reaction of $A + n \rightarrow B + \gamma$ at the center-of-mass energy E is proportional to :

$$\sigma^{\mu\nu}_{(n,\gamma)}(E, n) \propto \sum_{J,\pi}(2J+1) \cdot \frac{T^{\mu}_{n} T^{\nu}_{\gamma}}{T^{\mu}_{n} + T^{\nu}_{\gamma}} \tag{1}$$

where J is the half-integer neutron spin, T^{μ}_{n} and T^{ν}_{γ} are transmission coefficients i.e. the probability of penetration of the potential barrier. It reduced to : $\sigma^{\mu\nu}_{(n,\gamma)}(E_i, n) \sim T^{\nu}_{\gamma}$ because the energy of the incident neutron is $\sim$ KeV.

From the transmission coefficient to the Radiative Strenght Function (RSF)

The transmission coefficient for a photon of energy E_γ for a state μ in a given X-type, L-multipolarity transition is given by the following relation in terms of the RSF f_{XL} :

$$T_\gamma^\mu(E, J, \pi^\mu, E, J, \pi) = T_\gamma(E_\gamma; XL) = 2\pi f_{XL}(E_\gamma) E_\gamma^{2L+1} \quad (2)$$

The RSF for a X-type, L-multipolarity is given from the Bartholomew definition (Ref. [3]) :

$$f_{XL}(E_i, E_\gamma, \pi_i, J_i) = a_{XL} < B_{XL}(E_i, E_\gamma, \pi_i, J_i) > \rho(E_i) \quad (3)$$

With $< B_{XL}(E_i, E_\gamma, \pi_i, J_i) >$ being the mean over the excitation energies of reduced probability element in a bin of E_γ and $\rho(E_i)$ the density of state at the given excitation energy. The constant a_{XL} depends on the transition.

Nuclear Level Density

Let $N(E)$ be the number of levels up to an energy E. The nuclear level density (LD) is defined as :

$$\rho_{nucl}(E) = \frac{N(E+\Delta E) - N(E)}{\Delta E} \xrightarrow{\Delta E \to 0} \frac{\mathrm{d}N}{\mathrm{d}E} \tag{4}$$

The basic approach is to count the number of levels in the needed energy interval, ie. compute all the eigenvalues of the nuclear Hamiltonian and their degeneracy and then count how many fall into the interval $[E, E + \mathrm{d}E]$

γ-ray transitions in nuclei

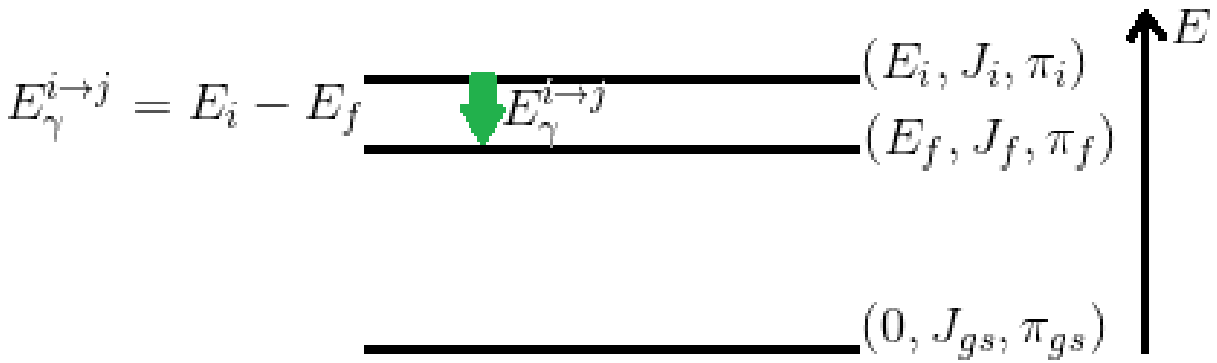

Figure 2: Scheme of a γ-transition

Characteristics of γ-rays : the carried momentum L and their type X (electric or magnetic). Given in function of the corresponding electric Q_L and magnetic M_L operators :

- $B(EL, J_i \to J_f) = \frac{1}{2J_i+1} |\langle f| |Q_L| |i\rangle|^2$
- $B(ML, J_i \to J_f) = \frac{1}{2J_i+1} |\langle f| |M_L| |i\rangle|^2$

No angular momentum information $\to$reduced matrix elements

Brink-Axel's hypothesis

Hypothesis

This is the assumption the cross section does not depend on the properties of the initial state $\leftrightarrow$ the RSF should not depend on the energy or the spin of the initial state.

Consequences

The absorption RSF built on an excited state can be approximated by the one built on the ground state. In that case, the Brink's hypothesis is equivalent to : $\overrightarrow{f} = \overleftarrow{f} = f$.

Nuclear Hamiltonian Problem

The microscopic Hamiltonian H in a non-relativistic model in which we assume that only two-body interactions are relevant takes the following form :

$$H = \sum_{ij} t_{ij} a_i^\dagger a_j + \frac{1}{4} \sum_{ijkl} \bar{v}_{ijkl} a_i^\dagger a_j^\dagger a_l a_k \tag{5}$$

Where the indices i, labeling single-particle states, goes from 0 up to ∞. The $\bar{v}_{ijkl}$ are the antisymmetrized matrix elements of the two-body interaction. The Hilbert Space is infinite $\rightarrow$need to be trimmed.

Nuclear Shell Model

One can consider two options :

- Restrict the number of particles and states (1)
- Approximate the eigentstates of H by simpler wave functions (2)

Shell Model is (1) : a phenomenological potential is added :

$$U(r) = \frac{1}{2} m\omega^2 r^2 + D \cdot \vec{l}^2 - C \cdot \vec{l} \cdot \vec{s} \tag{6}$$

We thus have : an isotropic harmonic oscillator potential, an orbit-orbit term and the spin-orbit coupling needed to reproduce the magic numbers (The first seven ones : 2, 8, 20, 28, 50, 82 and 126).

The Large Scale Shell Model

In this approach, we sunder the complete shell model of a nucleus into three parts :

- **The inert core :** orbits that are always full. They all have an energy which is under the Fermi energy.
- **The valence space :** part where we allow nucleon excitation.
- **The external space :** composed of the orbits that are always empty $\rightarrow$no allowed excitations here.

The **valence space**, is the basis for the calculations. We need to define an **effective interaction** which is designed for the valence space and a **numerical method** to diagonalize the Hamiltonian.

$E1$ transitions for ^{44}Sc

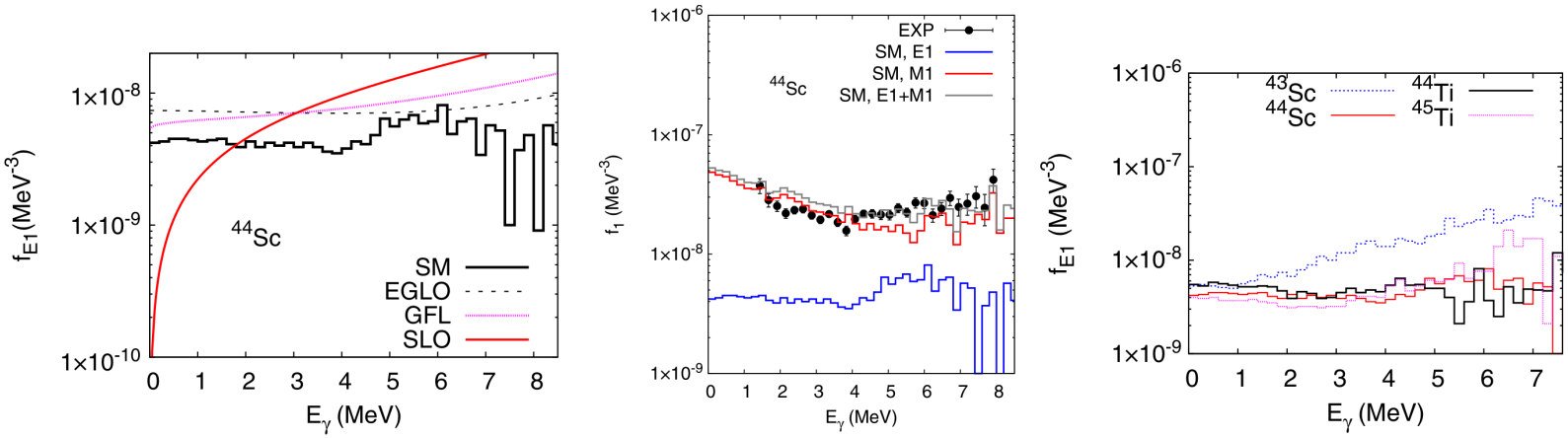

Figure 3: RSF of $E1$ transitions for ^{44}Sc taken from [5]

- Left : Computations with various model
- Center : Comparison with data
- Right : f_{E1} for other elements

$M1$ transitions for various Chromium and Titanium

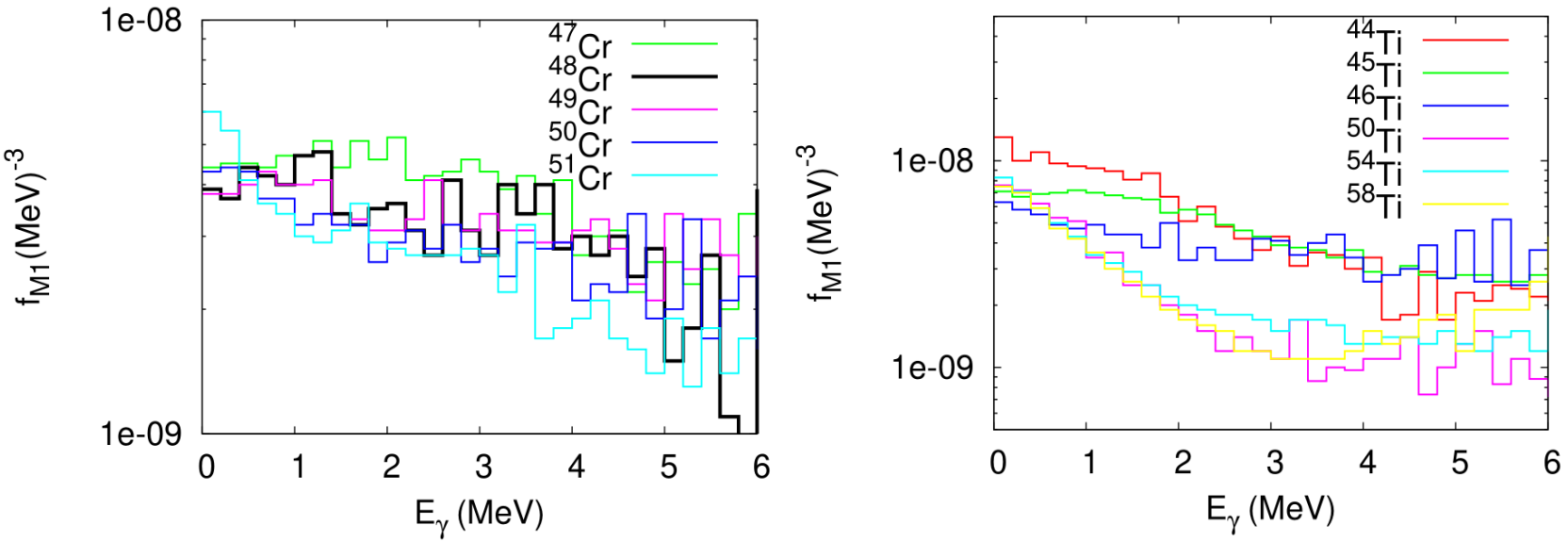

Figure 4: RSF of $M1$ transitions for various Chromium and Titanium taken from [2]

Goals

- Level Scheme to probe the shape of the nucleus.
- Compute the RSF for ^{48}Cr, ^{48}Ti and ^{50}Ti for $M1$ and $E2$ transitions.
- Look at the relevance of the shape of the nucleus with the shape of the RSF.
- Verify the Brink-Axel's hypothesis
- Find the configurations leading to the greatest transitions at low energies.

Yrast Band

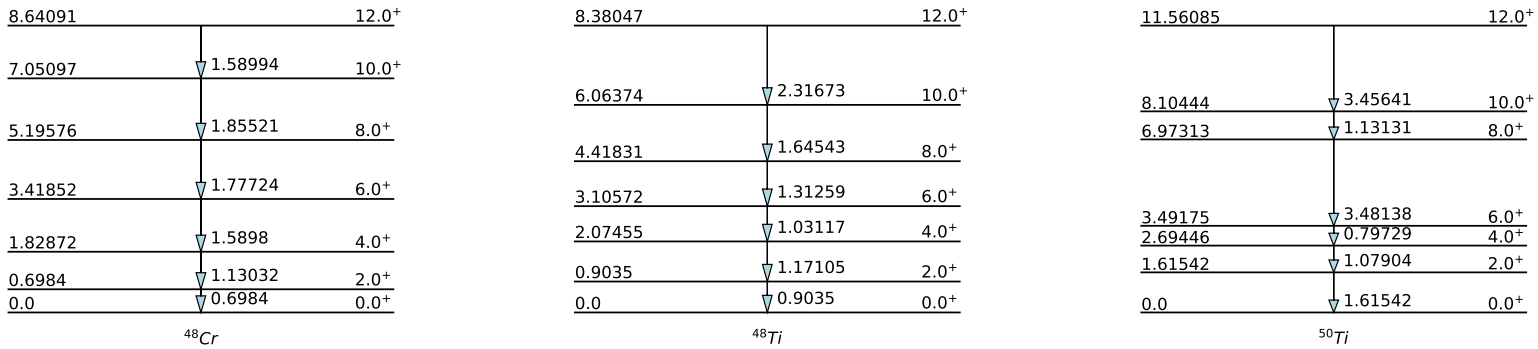

Figure 5: The levels scheme for the yrast of the three nuclei. The gap in excitation energy between two consecutives levels have been noted near the arrows. The excitation energy is in MeV.

$E_n = n\hbar\omega$ with n a natural number or $E = J(J+1)/\mathcal{J}$ where J is the spin and $\mathcal{J}$ is the moment of inertia of the nucleus.

Backbending

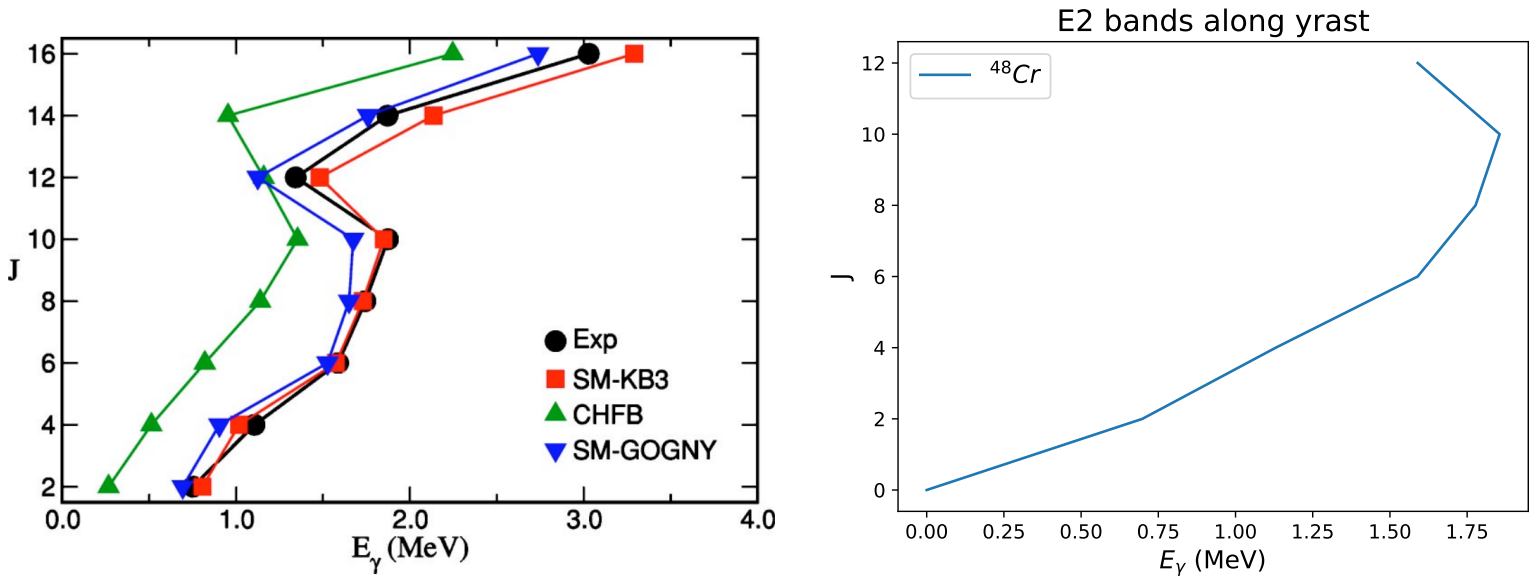

Figure 6: The backbending at $J = 12$ for ^{48}Cr, taken from [6] (left) and with the code written (right). The shape for $0 \leq J \leq 10$ indicates that ^{48}Cr is a good rotor.

RSF of $M1$ and $E2$ transitions

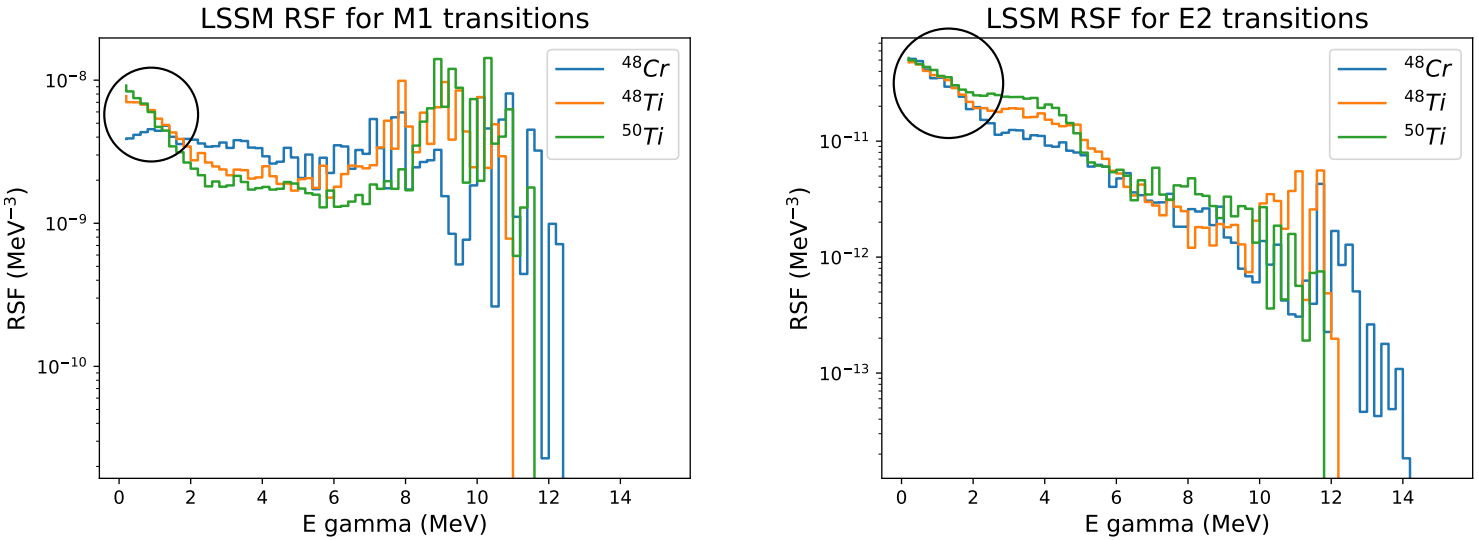

Figure 7: The RSF for $E2$ and $M1$ transitions obtained from shell-model calculations.

RSF of $M1$ transitions for various nuclei

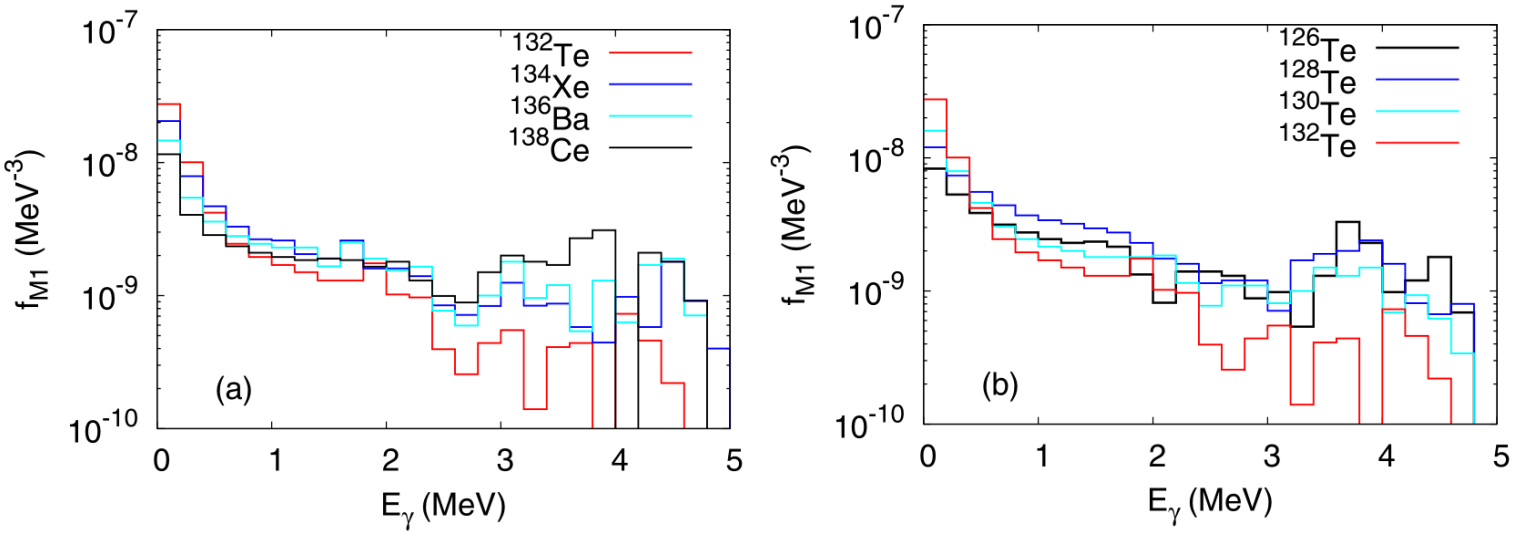

Figure 8: RSF of $M1$ transitions for various nuclei, taken from [1]

$E2$ transitions for Molybdenum

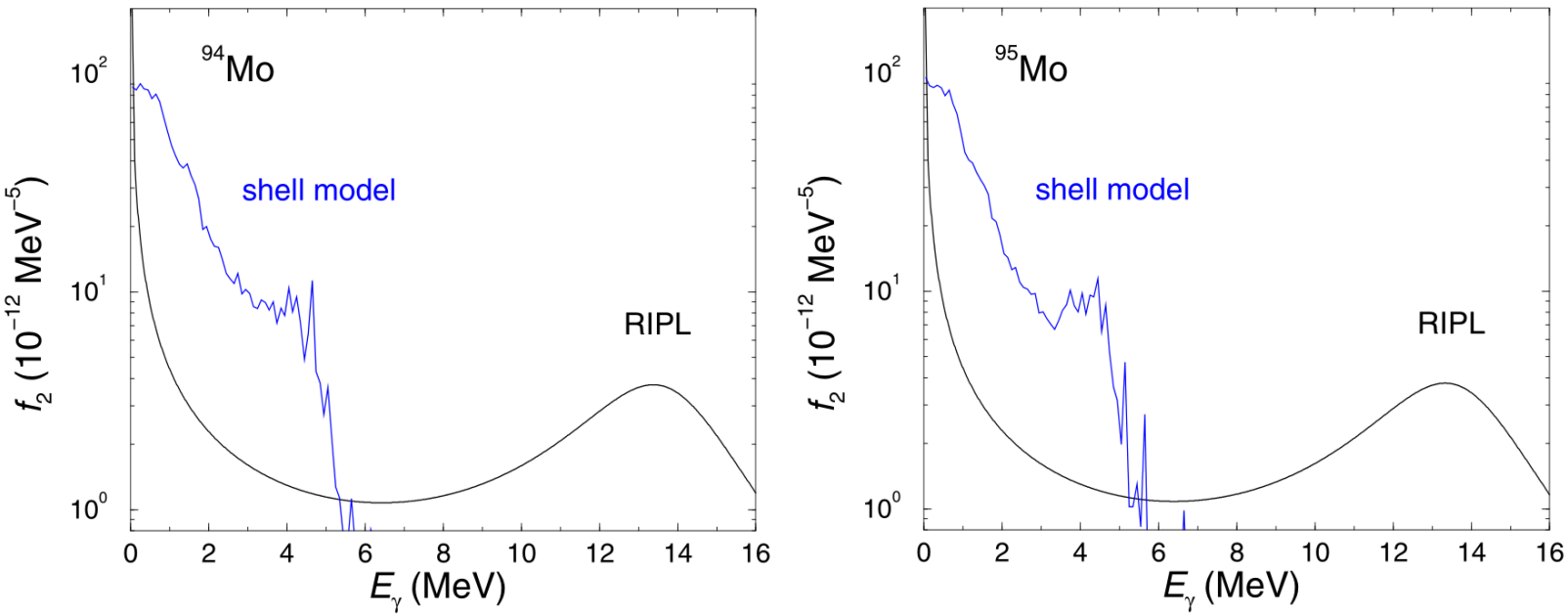

Figure 9: RSF of $E2$ transitions for ^{94}Mo and ^{95}Mo taken from [3]

Rotationnal Bands

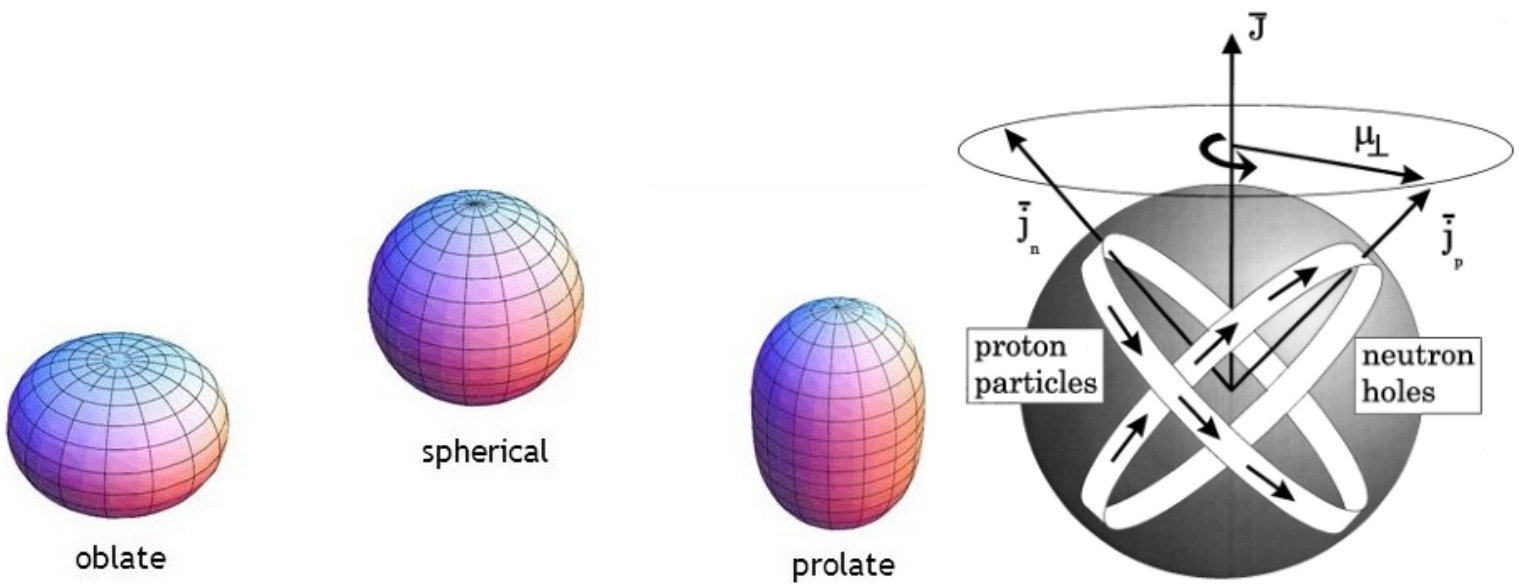

Figure 10: Left : quadrupole deformation ; Right : the shear mechanism. The angular momenta of the protons $\vec{j_p}$ and of the neutron holes $\vec{j_n}$ are separately lined-up. If they got aligned then the total momentum $\vec{J}$ will get larger. Figure taken from [4]

Presence of the shear mechanism in the nuclear chart

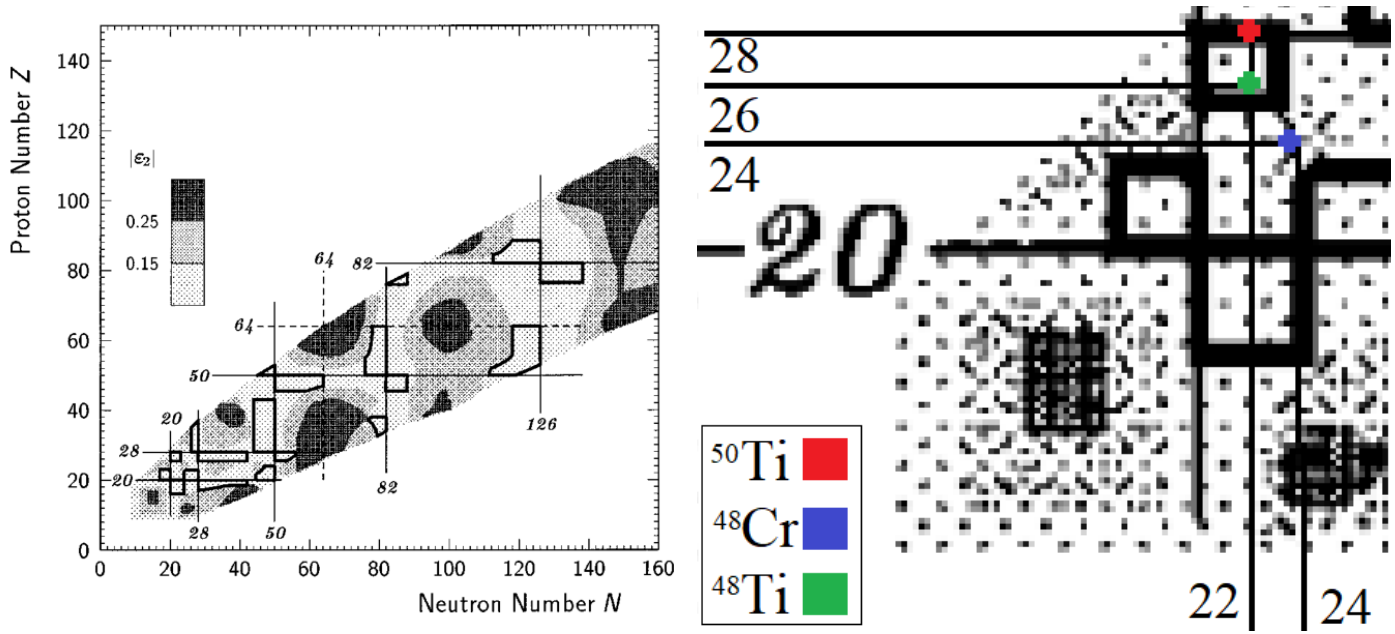

Figure 11: On the left, taken from [4] : predicted mass regions where magnetic rotation is possible. These regions are enclosed by thick solid lines ; on the right : zoom on the nuclei of this work

Testing the Brink-Axel's hypothesis

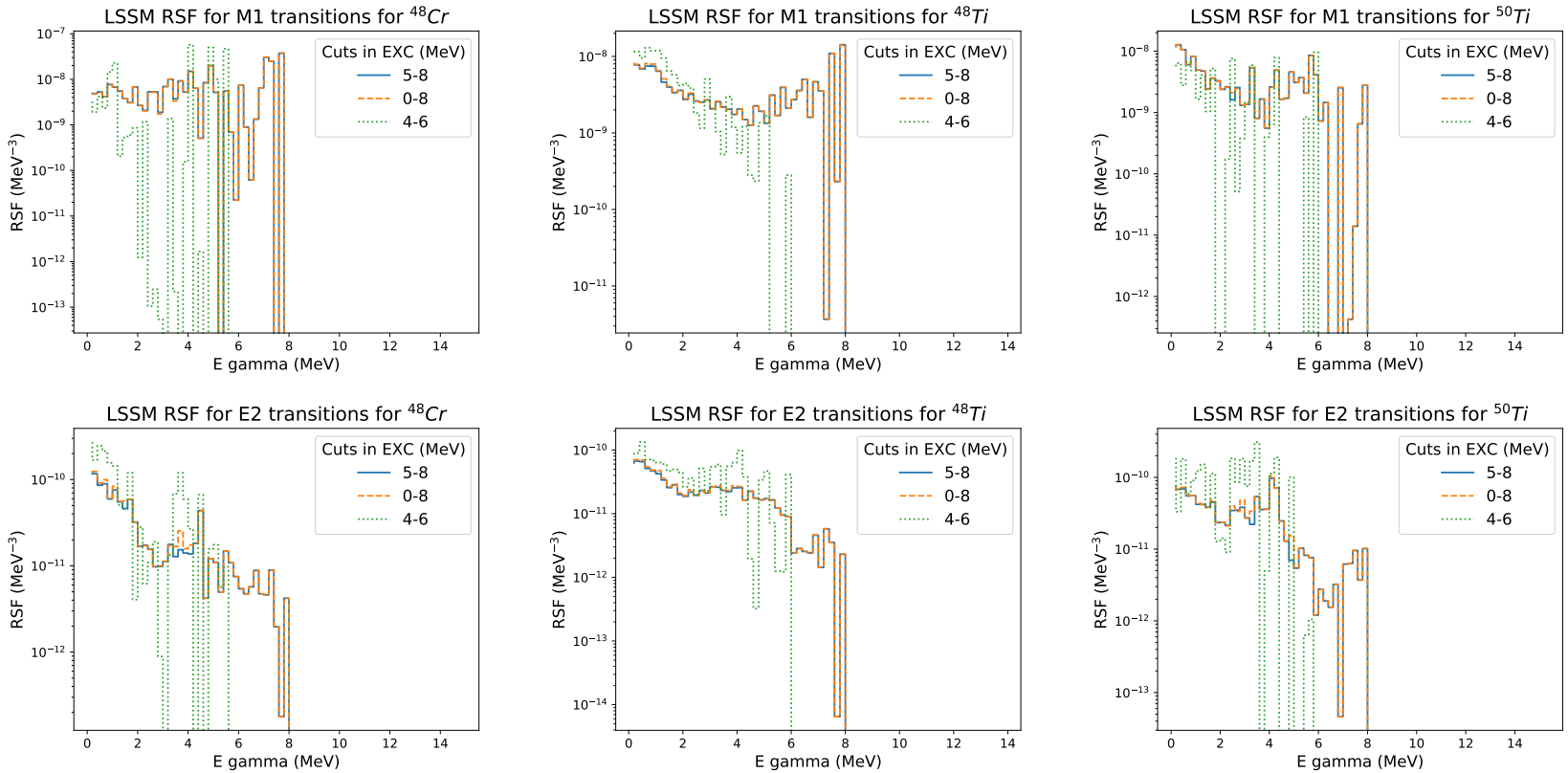

Figure 12: Plots of the $M1$ (upper line) and $E2$ (lower line) RSF for different cuts in excitation energy for the nuclei ^{48}Cr, ^{48}Ti and ^{50}Ti

Partial RSF

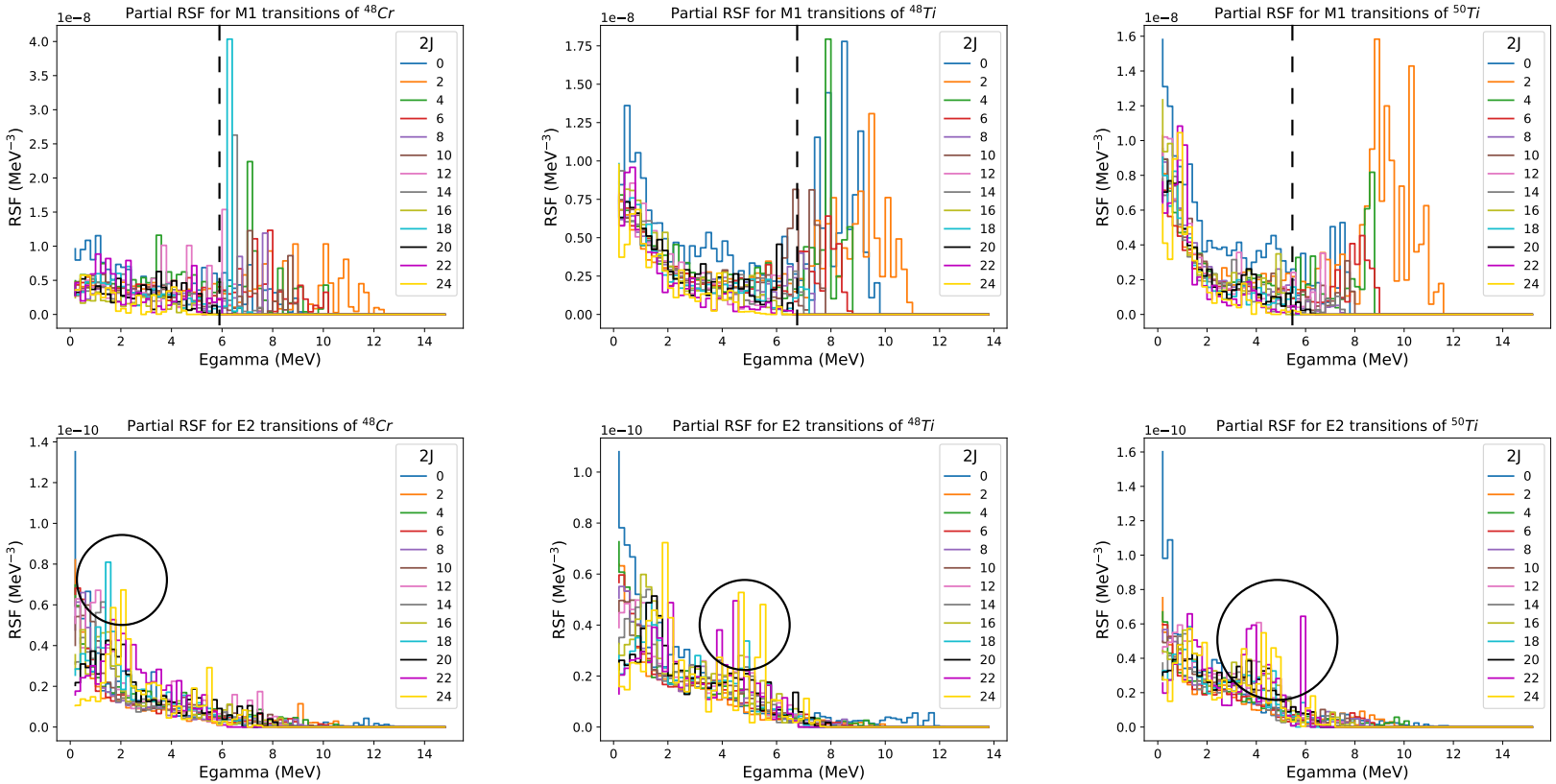

Figure 13: Partial $M1$ (upper line) and $E2$ (lower line) RSF for the nuclei ^{48}Cr, ^{48}Ti and ^{50}Ti

Main Configurations

The found states connected by the largest $B(XL)$:

$M1$ transitions

- ^{48}Cr : 4 p and 4 n on the $f7/2$ shell ; $J_f = J_i - 1$
- ^{50}Ti : 2 p on the $f7/2$ shell, 6-7 n on the $f5/2$ and 2-1 on the $p1/2$; $J_f = J_i - 1$
- ^{48}Ti : 2 p on the $f7/2$ shell and 6 n on the $f7/2$ shell ; $J_f = J_i \pm 1$

$E2$ transitions

- ^{48}Cr : 4 p and 4 n on the $f7/2$ shell ; $J_f = J_i - 2$
- ^{50}Ti : 2 p on the $f7/2$ shell, 6-7 n on the $f5/2$ and 2-1 on the $p1/2$; $J_f = J_i - 1$ $(0 < E_\gamma < 1)$ and $J_f = J_i - 2$ $(1 < E_\gamma < 2)$.
- ^{48}Ti : 2 p on the $f7/2$ shell and 6 n on the $f7/2$ shell ; $J_f = J_i \pm 1$; $J_f = J_i - 1$ $(0 < E_\gamma < 1)$ and $J_f = J_i - 2$ $(1 < E_\gamma < 2)$.

Conclusion

- We have compared the properties of the $E2$ RSF of three nuclei : ^{48}Cr, ^{50}Ti and ^{48}Ti. In three cases it has been to shown to provide very small effects when compared to the corresponding $M1$ transitions.
- The hypothesis made for the calculations, the Brink-Axel's hypothesis holds trues.
- There is an increase at low energies for all three nuclei which should differ from the RIPL formula.
- Presence of a spin-flip.
- The main connected configurations have been found and they differ from [3], only study on $E2$ transitions, albeit with other elements.

Bibliography

- Loens, Hans Peter. Microscopic radiative strength functions and fission barriers for r-process nucleosynthesis. Germany: PhD thesis, TU Darmstadt, 2011
- D.Rochman *et al.*, Phys. Lett. B (2016).
- G.A. Bartholomew, E.D. Earle, A.J. Ferguson, J.W. Knowles, and M.A. Lone. Adv. Nucl. Phys., 7:229, 1972.
- S. Frauendorf, Rev. Mod. Phys. 73, 463
- K.S. Krane,Introductory Nuclear Physics (Wiley, New York/Chichester/Brisbane/Toronto/Singapore) (1988).
- in Proceedings of the Workshop on Gamma Sphere Physics, Berkeley, edited by M.A. Dele- planque, I.Y. Lee, and A.O. Macchiavelli (World Scientific, Singapore), p. 272.

Bibliography

- S. Goriely, S. Hilaire, S. Péru, M. Martini, I. Deloncle, and F. Lechaftois, Phys. Rev. C 94, 044306 (2016)
- S. Goriely, S. Hilaire, S. Péru and K. Sieja, Phys. Rev. C 98, 014327 (2018)
- R. Schwengner, S. Frauendorf, and A. C. Larsen, Low-Energy Enhancement of Magnetic Dipole Radiation, Phys. Rev. Lett., 118:092502, 2013
- A. C. Larsen, J. E. Midtbø, M. Guttormsen, T. Renstrøm, S. N. Liddick, A. Spyrou, S. Karampagia, B. A. Brown, O. Achakovskiy, S. Kamerdzhiev, D. L. Bleuel, A. Couture, L. Crespo Campo, B. P. Crider, A. C. Dombos, R. Lewis, S. Mosby, F. Naqvi, G. Perdikakis, C. J. Prokop, S. J. Quinn, and S. Siem. Phys. Rev. C, 97:054329, May 2018.

Bibliography

- K.Sieja, Phys. Rev. C 98, 064312 (2018)
- K.Sieja & S. Goriely Recent shell-model calculations of gamma-decay strength functions, to appear in Acta Physics Polonica (2020)
- R. Schwengner, Phys. Rev. C 90,064321 (2014)
- https://www-nds.iaea.org/RIPL-3/
- E. Caurier, A. P. Zuker, A. Poves, and G. Martínez-Pinedo,Phys. Rev. C 50, 225 (1994)
- E. Caurier, G. Martínez-Pinedo, F. Nowacki, A. Poves, and A. P. Zuker, Rev. Mod. Phys. 77, 427 (2005)

Change of parity of the transitions

The selection rules are the following : $|J_i - J_f| \leq L \leq J_i + J_f$ for the angular momentum and $\pi_i = (-1)^L \pi_f$ or $\pi_i = (-1)^{L+1} \pi_f$ for the parity for electric transitions (respectively for magnetic transitions). The change of parity for L=1,2 and 3 is summarized in :

Table 1: The behavior the three first multipolarities for both electric and magnetic type transitions

Type \Multipolarity	1	2	3
Magnetic	No	Yes	No
Electric	Yes	No	Yes